

Atmospheric Drivers Associated with Extreme Snow Ablation and Discharge Events in the Susquehanna River Basin: A Climatology

ZACHARY J. SURIANO^a, GINA R. HENDERSON^b, JULIA ARTHUR^b, KRICKET HARPER^b, AND DANIEL J. LEATHERS^c

^a *Department of Earth, Environmental, and Atmospheric Sciences, Western Kentucky University, Bowling Green, Kentucky*

^b *Department of Ocean and Atmospheric Sciences, U.S. Naval Academy, Annapolis, Maryland*

^c *Department of Geography and Spatial Sciences, University of Delaware, Newark, Delaware*

(Manuscript received 6 March 2023, in final form 7 July 2023, accepted 19 September 2023)

ABSTRACT: Extreme snow ablation can greatly impact regional hydrology, affecting streamflow, soil moisture, and groundwater supplies. Relatively little is known about the climatology of extreme ablation events in the eastern United States, and the causal atmospheric forcing mechanisms behind such events. Studying the Susquehanna River basin over a 50-yr period, here we evaluate the variability of extreme ablation and river discharge events in conjunction with a synoptic classification and global-scale teleconnection pattern analysis. Results indicate that an average of 4.2 extreme ablation events occurred within the basin per year, where some 88% of those events resulted in an increase in river discharge when evaluated at a 3-day lag. Both extreme ablation and extreme discharge events occurred most frequently during instances of southerly synoptic-scale flow, accounting for 35.7% and 35.8% of events, respectively. However, extreme ablation was also regularly observed during high pressure overhead and rain-on-snow synoptic weather types. The largest magnitude of snow ablation per extreme event occurred during occasions of rain-on-snow, where a basinwide, areal-weighted 5.7 cm of snow depth was lost, approximately 23% larger than the average extreme event. Interannually, southerly flow synoptic weather types were more frequent during winter seasons when the Arctic and North Atlantic Oscillations were positively phased. Approximately 30% of the variance in rain-on-snow weather type frequency was explained by the Pacific–North American pattern. Evaluating the pathway of physical forcing mechanisms from regional events up through global patterns allows for improved understanding of the processes resulting in extreme ablation and discharge across the Susquehanna basin.

SIGNIFICANCE STATEMENT: The purpose of this study is to better understand how certain weather patterns are related to extreme snowmelt and streamflow events and what causes those weather patterns to vary with time. This is valuable information for informing hazard preparation and resource management within the basin. We found that weather patterns with southerly winds were the most frequent patterns responsible for extreme melt and streamflow, and those patterns occurred more often when the Arctic and North Atlantic Oscillations were in their “positive” configuration. Future work should consider the potential for these patterns, and related impacts, to change over time.

KEYWORDS: North America; Synoptic climatology; Teleconnections; Snowmelt/icemelt; Streamflow

1. Introduction

Snow ablation is critically important to the hydroclimatology of any watershed with snowpack in its seasonal cycle (Fritze et al. 2011). Both the frequency and magnitude of rapid ablation events not only affect variables such as soil moisture and groundwater supply within a watershed, but can also lead to increased streamflow and potentially flooding (Barnett et al. 2005). To date, the vast majority of snow ablation research in the United States has occurred in the western third of the country, where deep and long-lived seasonal

snowpacks exist in mountainous environments. Prior research in this western region has evaluated snowpack and ablation climatologies (P. W. Mote et al. 2018; Welty and Zeng 2021; Haleakala et al. 2021), rain-on-snow ablation (McCabe et al. 2007; Mazurkiewicz et al. 2008; Cohen et al. 2015; Guan et al. 2016), trends in snow and snowmelt (Fritze et al. 2011; Siirila-Woodburn et al. 2021), and hydrologic implications of varying and changing snow (Yan et al. 2019; Li et al. 2017; Hatchett et al. 2022; Musselman et al. 2021), among other areas of emphasis. In contrast, the highly ephemeral and relatively thin snowpacks of the eastern United States are understudied despite the role snow ablation plays in influencing water resources (Frei et al. 2002; Pradhanang et al. 2011) and their potential for hazardous events (Yarnal et al. 1997). This study focuses on snow ablation and associated discharge in the Susquehanna River basin (SRB) within the eastern United States.

In the mid-Atlantic region of the United States, the SRB has a 110-day average snow season, typically from early December through late March, where snow depths average 8.8 cm (Suriano et al. 2020). It is common for the snowpack to accumulate and completely ablate on multiple occasions during a snow season. Such ephemeral snow cover leads to multiple instances of

Denotes content that is immediately available upon publication as open access.

Supplemental information related to this paper is available at the Journals Online website: <https://doi.org/10.1175/JAMC-D-23-0042.s1>.

Corresponding author: Zachary J. Suriano, zachary.suriano@wku.edu

DOI: 10.1175/JAMC-D-23-0042.1

© 2023 American Meteorological Society. This published article is licensed under the terms of the default AMS reuse license. For information regarding reuse of this content and general copyright information, consult the AMS Copyright Policy (www.ametsoc.org/PUBSReuseLicenses).

snowmelt-induced runoff each year, as compared with a single large event that is the norm for many more northern and western regions. Furthermore, because of the high prominence of meteorological conditions suitable for snow ablation throughout the snow season (Leathers et al. 2004), the SRB is particularly susceptible to hazardous snowmelt-induced flooding. In the United States, a major snowmelt flood occurred more than once per year from 1972 to 2006, causing an average of \$68 million in damage (2007 dollars; Changnon 2008). In comparison, the most recognized SRB snowmelt flooding event occurred in January 1996, where there were nearly 30 fatalities, numerous injuries, and approximately \$1.5 billion in damage associated with the 2-day ablation of more than 50 cm of snow (10–15 cm SWE) with more than 7.5 cm of liquid precipitation (Yarnal et al. 1997; Leathers et al. 1998).

Hydrologically, the SRB supplies 90% of the total freshwater input in the upper Chesapeake Basin and over 50% of the entire basin input (Leathers et al. 2008). Variability in the discharge into the Chesapeake Bay has been linked to ecological complications due to transport of excess nutrients and pollutants (Anderson et al. 2002) and can also influence the generation of hydroelectric power and water management practices within the basin. Prior research has indicated the frequency and magnitude of snow depth change and river discharge change within the SRB are significantly positively correlated, particularly in December, where an increase in discharge of approximately $14\,310\text{ ft}^3\text{ s}^{-1}$ ($1\text{ ft}^3 \approx 0.03\text{ m}^3$) is observed for every 1.0 cm of snow depth loss (Suriano et al. 2020). On average, snow ablation events resulted in an increase in discharge of 155% over a 3-day lag, with the interannual frequency of discharge-causing snow ablation events significantly decreasing in the late twentieth century by approximately 45% (Suriano et al. 2020). What remains unclear within the SRB is which atmospheric mechanisms are associated with snow ablation and associated discharge and how global-scale patterns can influence regional and local-scale hydroclimatic outcomes.

The likelihood of an ablation event is dependent on the presence of snow cover and the occurrence of atmospheric patterns that provide sufficient meteorological conditions for melt (Grundstein and Leathers 1999). To examine the atmospheric setup and begin evaluating its influence on the snowpack, researchers may utilize synoptic classification techniques to establish days exhibiting similar atmospheric conditions under an individual synoptic weather type (Yarnal 1993). Each synoptic weather type modifies the snowpack in a different manner and can be used to link atmospheric forcings to ablation and streamflow. In midlatitude regions of the Northern Hemisphere, snow ablation typically occurs when there is southwesterly flow and advection of warm and potentially moist air into the region, including those that lead to rain-on-snow precipitation (Grundstein and Leathers 1999; McCabe et al. 2007; Mazurkiewicz et al. 2008; Bednorz 2009; Guan et al. 2016; Wachowicz et al. 2020). Ablation may also occur during other atmospheric conditions such as clear-sky days associated with a high pressure center (Suriano and Leathers 2018).

The goal of this study is to develop causal linkages between the occurrence of rapid snow ablation events and their corresponding streamflow discharges and the synoptic-scale forcings

within the watershed associated with both. By connecting synoptic-scale atmospheric circulation to the local hydrology, particular synoptic conditions that typically lead to ablation and instances of large streamflow can be identified, and improvements to flood forecasts and preparations can be made. Specific objectives are to (i) present a climatology of extreme snow ablation events and stream discharge events, by magnitude, for the SRB, (ii) determine the primary synoptic-scale weather patterns responsible for extreme snow ablation and discharge, and (iii) quantify the relationship between the interannual frequency of extreme ablation- and discharge-causing synoptic weather types and major large-scale teleconnection indices known to influence North America. To determine the synoptic-scale forcings of snow ablation, this study employs a temporal synoptic index (TSI; Kalkstein and Corrigan 1986) classification technique to create a daily calendar of synoptic conditions that can be examined in conjunction with snow ablation and discharge events.

2. Data and method

a. Study area

The SRB drains 71 210 km² across the states of New York, Pennsylvania, and Maryland in its 715-km path from Otsego Lake, New York, to Havre de Grace, Maryland, where it enters Chesapeake Bay (Fig. 1). Elevations across the watershed range from 954 m in the southwest portion of the basin to sea level as the river enters Chesapeake Bay (Fig. 1). The basin is home to over 4 million people, and its land cover currently consists of 62% natural vegetation (mostly forest), 25% cultivated vegetation, 10% developed lands, and 3% water bodies (<https://www.srb.net>). Since the beginning of European settlement in approximately 1700, the SRB has seen dramatic land-cover changes. The pre-European forested landscape was cleared first for agriculture, and later in the nineteenth century for production of lumber (Leathers et al. 2008). The lumbering resulted in the removal of the majority of hemlock (*Tsuga Canadensis* L.) and white pine (*Pinus strobes* L.) from the basin (Leathers et al. 2008). In the last century, much of the original portions of the watershed clear-cut for lumber have seen natural regeneration, but the reforested landscape is different, containing primarily hardwood species. The entire SRB is prone to flooding, and flood damages average \$150 million per year (<https://www.srb.net>). In the past, major floods in the basin have been caused by diverse mechanisms ranging from snow-cover ablation to heavy precipitation caused by tropical cyclones.

As noted previously, the SRB is the primary contributor to the freshwater flow within the Chesapeake Bay. Additionally, snow receipts from the James and Potomac River basins are relatively small in comparison with those of the SRB. Because of the dominance of the SRB in the overall Chesapeake discharge (Fig. 2) and basin snow cover, parallels can be drawn from the atmospheric forcings affecting ablation within the SRB to those affecting the larger Chesapeake Basin.

b. Extreme ablation data, definition, and calculation

Daily snow depth data used in calculating ablation for the SRB (approximately 40.5°–42.5°N, 75.5°–78.5°W) for the period

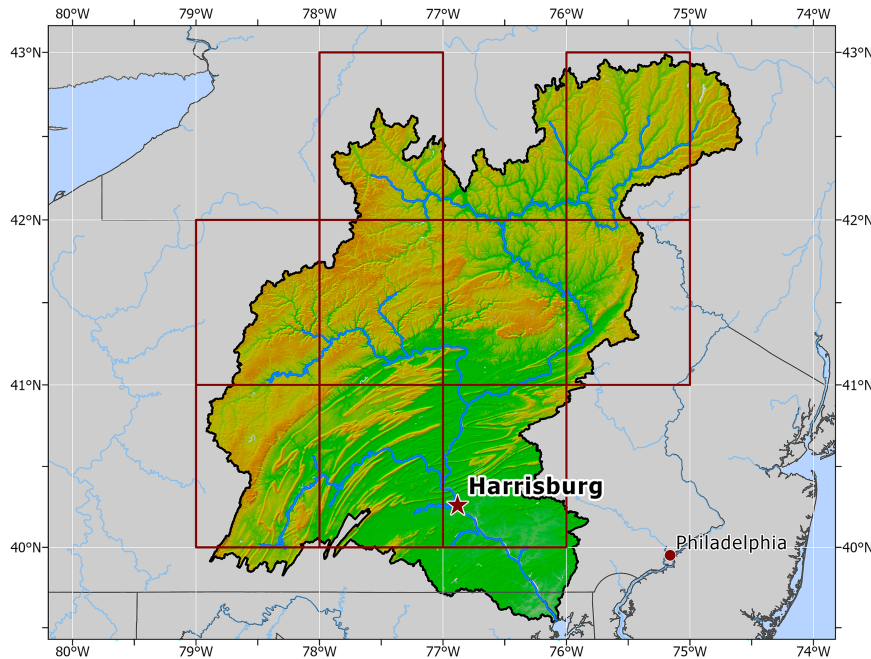


FIG. 1. SRB topography and basin boundary representation at a 1° gridded resolution (dark-outlined grid cells). Harrisburg is the location of the river discharge station used in the study, and Philadelphia is the station used in the TSI classification.

1960–2009 were obtained from the Daily Gridded North American Snow, Temperature, and Precipitation dataset (T. L. Mote et al. 2018). The SRB at the dataset's 1° latitude \times longitude resolution was determined based on a centroid method, where only the grid cells in which the cells' centroid fell within the geographical boundaries of the basin were included. Based on the U.S. Geological Survey (USGS) Water Boundary Dataset (<http://nhd.usgs.gov/wbd.html>), the SRB consisted of nine 1° grid cells (Fig. 1).

The gridded snow dataset is available for a majority of the North American landmass and is based on in situ observations from the National Weather Service Cooperative Observer Program and the Meteorological Service of Canada network. The dataset has undergone extensive quality control routines (Robinson 1988; Suriano and Leathers 2017) and has been validated through stratified sampling and k -fold cross-validation analyses (Kluver et al. 2017). Station density was sufficient for analysis within the SRB, with many cells reporting over 10 station

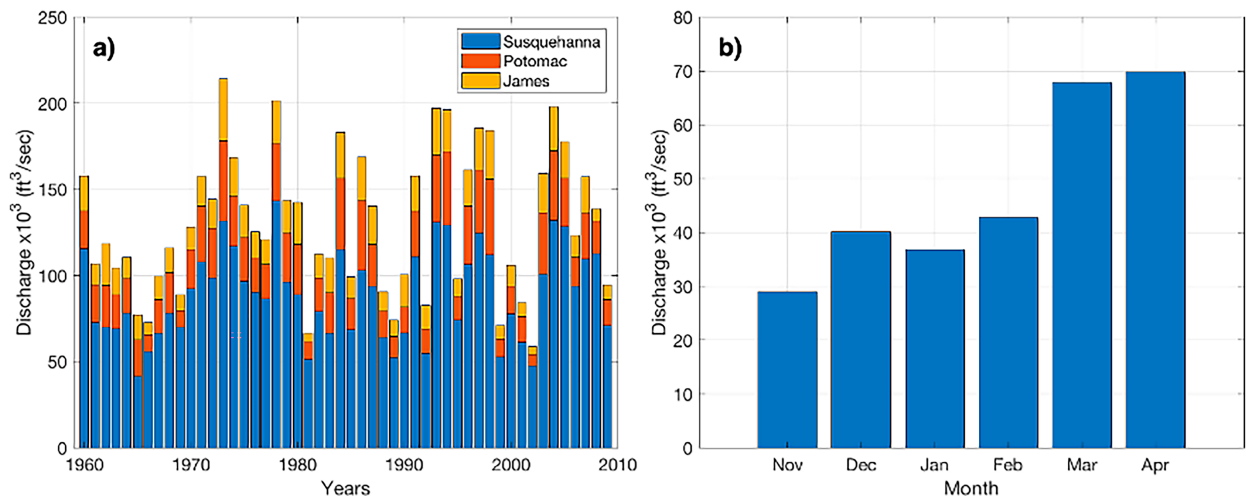


FIG. 2. (a) Stream discharge ($\times 10^3 \text{ ft}^3 \text{ s}^{-1}$) interannually during the November–April study season for the Susquehanna (blue), Potomac (orange), and James (yellow) Rivers, and (b) mean monthly stream discharge ($\times 10^3 \text{ ft}^3 \text{ s}^{-1}$) for the Susquehanna River only.

observations daily (Kliver et al. 2017). These data are currently available online at the National Snow and Ice Data Center (<http://nsidc.org/data/G10021>).

The Daily Gridded North American Snow, Temperature, and Precipitation dataset was suitable for this application due to its consistent use of observations from the Cooperative Observer Program in the United States and its long period of record. While other data products were considered, the use of snow observations, not modeled or reanalyzed products, was preferred, and the selected dataset allowed for the climatological perspective necessary for this study, despite the dataset's termination in 2009. This is discussed in greater lengths within the limitations section (section 2e).

Snow ablation events were defined as an interdiurnal decrease in areal-weighted average snow depth across the SRB. To focus only on ablation with the most potential for societal impact, only events within the top 5% of the distribution of depth change magnitude were analyzed, corresponding to a depth decrease of 3.0 cm. These events are designated here as extreme. Further, events were only analyzed when (i) the maximum temperature on the second day of the associated interdiurnal event exceeded 0°C (Dyer and Mote 2007) and (ii) when no new snowfall accumulations greater than 2.54 cm were recorded on any of the 3 days preceding the event (Suriano and Leathers 2018). These criteria aid in removing the effect of snowpack compaction as effectively as possible from daily snow depth measurements. In contrast to deep mountain snowpacks, under such conditions in ephemeral snow environments, the snowpack can be assumed to be relatively isothermal and mature (Dyer and Mote 2007). After 3 days of no new substantial snow accumulations, the impact of snow compaction at the given depth change threshold would be nominal and is based on estimated snow-density calculations (Anderson 1976; Suriano and Leathers 2018). This definition of snow ablation does not account for snow depth changes that are the result of sublimation, as this effect is generally minimal for a single event (Dèry and Yau 2002). The authors acknowledge a small portion of daily snow depth decreases could be attributable to sublimation. Prior research has shown this methodological approach to be a valid proxy for detecting snow ablation without the use of snow mass or snow water equivalent (Leathers et al. 2004; Dyer and Mote 2007; Suriano and Leathers 2018, among others), where statistically significant relationships between depth change and discharge exist (Suriano et al. 2020).

As identified in Suriano and Leathers (2017), changes in the number of reporting observation stations can influence an interpolated interdiurnal snow depth change for a grid cell. To ensure high fidelity of the snow depth data, days and grid cells identified in the quality control routines of Suriano and Leathers (2017) as suspicious were removed from analysis. This may create the potential for an areal-weighted average snow depth for the basin to be based on different areas (i.e., different number of grid cells) over successive days. As such, a threshold of daily grid cells reporting was applied. With nine total grid cells composing the SRB (Fig. 1), only days with at least eight of nine grid cells reporting were considered (i.e., 89% of cells), resulting in 97.8% of the possible ablation events being available for analysis. The average ablation magnitude

was not significantly different between events with an 89% (eight of nine cells required) and 100% (nine of nine cells required) threshold.

c. Extreme discharge data, definition, and calculation

Daily stream discharge for the SRB for the years 1960–2009 was collected from the USGS streamflow gauge network at Harrisburg, Pennsylvania (USGS 01570500; see Fig. 1). The Harrisburg gauge site was the farthest station downstream before major dams and had minimal missing data (<1%) over the 50-yr period of record, making it the most suitable for this analysis.

Here, a discharge event is defined as an interdiurnal increase in discharge at a 3-day lag (Suriano et al. 2020). For instance, a discharge event was equivalent to the discharge on day 3 minus the discharge on day zero. Peak lag in discharge was determined by cross-correlation analysis to occur between 2 and 4 days after an associated ablation event (Suriano et al. 2020). However, beyond 3 days, the influence of a particular synoptic weather type on discharge becomes indiscernible from the impact of the next synoptic-scale system. Thus, this study will focus on the 3-day lag in discharge associated with snow ablation. Similar to the ablation analysis, only discharge events in the top 5% of the September–August distribution by magnitude were analyzed. This corresponds to a 3-day increase in discharge of $86\,000\text{ ft}^3\text{ s}^{-1}$. Discharge events at or above this threshold are considered as extreme in this study.

A number of environmental variables influence the relationship between ablation and discharge beyond decreases in snow depth, including snowpack density and temperature, ground saturation, soil characteristics, and additions of liquid precipitation. Because of these other factors, it is not expected for there to be a streamflow response associated with every ablation event within the basin. However, previous work has noted that approximately 75% of ablation events result in a positive (increasing) response in river discharge at a 3-day lag in the Susquehanna River, where ablation magnitude is significantly related to the magnitude of discharge response (Suriano et al. 2020). Snow ablation events and associated river discharge responses were initially examined over the entire September through August snow season. However, with no ablation events occurring in the warm season, analysis was restricted to November through April during the period 1960–2009.

d. Synoptic classification

Daily synoptic weather types were developed using the TSI synoptic-typing methodology (Kalkstein and Corrigan 1986), based on meteorological data in Philadelphia, Pennsylvania [Weather Bureau Army–Navy (WBAN) 13739, 39.87°N, 75.23°W]. Such a synoptic weather-typing technique represents days with similar atmospheric conditions as a single weather type, which facilitates the evaluation of the atmosphere's influence on the underlying surface (Yarnal 1993). In this study, synoptic weather typing is used to determine the relationship between basin-scale snow ablation and synoptic-scale circulation and to track the frequency of synoptic types in which long-term changes can alter the climate.

Meteorological observations from 1960 to 2009 for Philadelphia were obtained from the National Centers for Environmental Information (NCEI) for the TSI at four daily observation periods (0900, 1500, 2100, and 0300 UTC). Data include temperature, dewpoint temperature, sea level pressure, surface wind vectors, and cloud cover. An unrotated P-mode principal components analysis was conducted on the 4-times-daily meteorological observations to identify the principal components with eigenvalues greater than 1.0 for each climatological season [autumn (SON), winter (DJF), and spring (MAM)]. Summer (JJA) was not included because of a lack of snow cover in the SRB during this time of year. Such climatological season classifications are preferred over a single annual classification because this limits the influence of the annual cycle on the explained variance of the PCA (Siegert et al. 2017).

Five principal components were retained each season, explaining approximately 79.3%–81.0% of seasonal variance. The five principal components align well with (i) the air mass, (ii) the configuration of the sea level pressure field relative to Philadelphia, and (iii) the daily progression of cloud cover, and the direction and strength of the (iv) zonal and (v) meridional wind fields. The seasonal component scores, the weighted sums of the original variable by the component loading, are then clustered using within-group average linkage clustering with an initial 20-cluster solution. Within-group average linkage is identified as the most appropriate clustering method for the TSI (Kalkstein et al. 1987). The TSI of this study differs from that of Kalkstein and Corrigan (1986) because of the use of the preferred within-group average linkage, as compared with the original Ward's clustering.

A qualitative assessment of each season's initial 20 cluster solutions, or synoptic weather types, was then performed using the approach described in Siegert et al. (2021). Composites of sea level pressure and 500-hPa geopotential height fields were generated for each synoptic weather type using NCEP–NCAR Reanalysis 1 (Kalnay et al. 1996). This allows for each type to be categorized into general synoptic weather categories (SWCs) relative to the SRB: high pressure overhead, northwesterly flow, southerly flow, and weak flow (Suriano 2020). While not necessarily a dominant synoptic-scale flow regime, a fifth SWC of rain-on-snow was established in line with previous literature (Suriano and Leathers 2018; Suriano 2020) to examine the impact of rain-on-snow ablation within the region (see Wachowicz et al. 2020). Further discussion of the sea level pressure fields and resulting impacts to ablation are discussed within the results section. The result of the procedure was a daily synoptic calendar where each day is represented by an individual SWC over the 50-yr period. While other newer reanalysis products, for example, ERA5, may have been able to provide a finer-scale spatial resolution than NCEP–NCAR Reanalysis 1, for the specific variables examined here, it provides sufficient resolution. Further, sea level pressure and 500-hPa heights are among the variables most strongly influenced by observed data (Kalnay et al. 1996). With a high observation station density in the U.S. mid-Atlantic/Northeast during the study period, model bias is likely reduced relative to sparsely observed regions (Lindsay et al. 2013). This indicates that these variables

are considered the most reliable for analysis, and thus NCEP–NCAR Reanalysis 1 is appropriate for this specific application.

The identified basinwide average ablation events and discharge responses for the SRB were examined in conjunction with the daily synoptic calendar to isolate the frequency and magnitude of ablation associated with each synoptic category. Only synoptic weather types that represented a relative frequency of at least 2% of the extreme ablation events, extreme discharge events, and/or total November–April days were retained. This restriction helps to simplify analysis, limiting discussion to only the 27 most impactful synoptic weather types, which were binned into their corresponding SWC. A climatology of extreme snow ablation events and discharge responses is presented followed by a detailed analysis of the SWCs' relationships to these variables.

To evaluate possible forcing mechanisms of the synoptic weather types' frequencies over time, the role of large-scale atmospheric and oceanic modes of variability, that is, teleconnections, was examined. Teleconnection indices known to influence the broader region were isolated at monthly time scales, detrended to remove any long-term systematic movements away from the mean, and correlated against the weather types' frequencies at seasonal scales. Teleconnection indices used were the Arctic Oscillation (AO; Higgins et al. 2000), North Atlantic Oscillation (NAO; Barnston and Livezey 1987), Pacific–North American pattern (PNA; Leathers et al. 1991), Pacific decadal oscillation (PDO; Zhang et al. 1997), Niño-3.4 ENSO index, and Atlantic multidecadal oscillation (AMO; Enfield et al. 2001). Data were obtained from NOAA's Physical Sciences Laboratory.

e. Limitations

One of the primary limitations of this study is the termination of the snow depth dataset in 2009. Such a termination date effectively prohibits a robust temporal investigation of extreme ablation events within the basin. While such an objective would have added value to the analysis, specific care was taken to not speak to change or variation over time, but rather to focus on the climatological period and the role of synoptic and global-scale circulation and their influence on events. Other datasets were initially considered, such as the Daily 4-km Gridded SWE and Snow Depth (Broxton et al. 2019) and the Snow Data Assimilation System (SNODAS). Despite both of these datasets providing current data, the decision to use the $1^\circ \times 1^\circ$ gridded dataset (T. L. Mote et al. 2018) was driven by the long-term nature of the dataset and its consistent use of COOP observations. For instance, SNODAS currently has coverage starting in 2003 and would prove insufficient in capturing the long-term variability sought in this study. Further, the Daily 4-km Gridded SWE product (Broxton et al. 2019) heavily incorporates SNOTEL stations in the mountain west into its algorithms. With the lack of SNOTEL measurements in the central and eastern United States, there are concerns about the product's performance in the SRB.

Second, there are inherent limitations to the synoptic classification technique used here, specifically the binning of weather types into SWCs. These general categories are broad by design

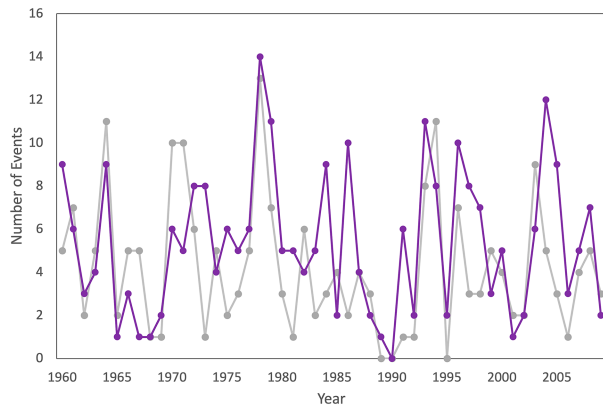


FIG. 3. Interannual frequency of extreme (top 5%) November–April daily snow ablation (gray) and stream discharge (purple) events for the SRB.

and serve to simplify analysis. However, the placement of individual synoptic weather types (i.e., cluster solutions) into an SWC is subjective and prone to potential variations based on researcher biases. The reclassification of an individual weather type into a different SWC may result in a change in the general conclusions found here, and while similar at a synoptic scale, individual types within an SWC may exhibit a range of smaller-scale features. As such, care was taken in assigning individual types to an SWC following the principles outlined in Siegart et al. (2021).

3. Results

a. Climatology of extreme ablation and discharge events

Across the 50-yr study period, approximately 4.2 extreme ablation events occurred per November–April season [standard deviation (SD): 3.1 events per year], with a maximum of 13 events in the period 1977/78, and a minimum of 0 events in

1988/89, 1989/90, and 1994/95 (Fig. 3). On average, an extreme ablation event results in an areal-weighted basinwide snow depth decrease of 4.5 cm (SD: 1.6 cm). A seasonal distribution of the SRB extreme ablation events indicates a majority of events occur during the months of February and March, contributing 31.8% and 28.9% of the total events, respectively (Fig. 4a; Table 1). Within the basin, the largest ablation events typically occur in the northern regions, and ablation magnitude during a basinwide event is not necessarily spatially homogenous (Fig. 5). Approximately 87.7% of extreme ablation events are observed in conjunction with a discharge event at a 3-day lag (i.e., increase in discharge). In comparison, 27.5% of extreme ablation events occurred in conjunction with an extreme discharge event (i.e., top 5% of discharge events) at the same lag.

A total of 332 three-day-lag discharge events met the threshold for extreme over the 50-yr period, inclusive of the entire calendar year. Of those, 80.8% occurred during the November–April study season, for an average of 5.0 extreme events per season (SD: 3.3), showcasing the importance of snow processes in the hydrology of the basin. Maximum frequency occurred in 1977/78, with 14 extreme discharge events, while a minimum frequency of 0 extreme events occurred in 1989/90 (Fig. 3). On average, an extreme discharge event resulted in an increase in discharge of $141\,383\text{ ft}^3\text{ s}^{-1}$ (SD: $59\,796\text{ ft}^3\text{ s}^{-1}$) over the 3-day lag. The seasonal distribution of extreme discharge events indicates March, followed by February, have the greatest frequency at 31.0% and 18.7%, respectively, aligning with the maximum frequency of extreme ablation within the basin (Fig. 4b). For 52.7% of extreme discharge events, a snow ablation event occurred 3 days prior (i.e., a 3 day lag), with 17.5% of all extreme discharge events being associated with an extreme ablation event 3 days prior.

b. Synoptic weather types

The synoptic weather types categorized into the five SWCs represent approximately 81% of all November–April days from 1960 to 2009. Representative sea level pressure patterns

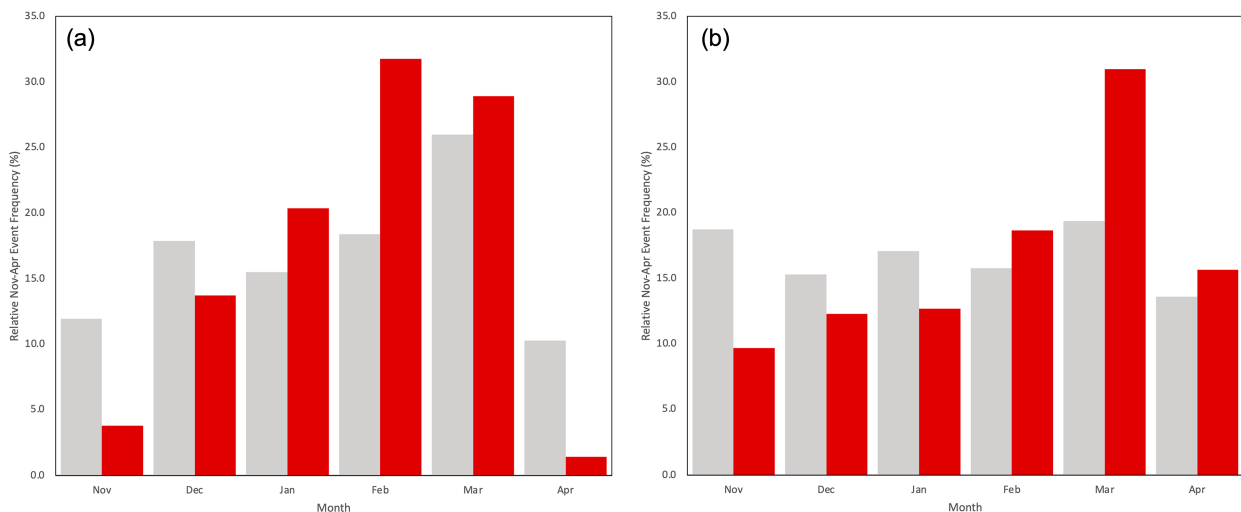


FIG. 4. Monthly relative frequency (%) of all events (gray bars) and extreme events (red bars) from 1960 to 2009 for (a) snow ablation events and (b) stream discharge events.

TABLE 1. Monthly ablation frequency for the SRB for November–April. Ablation event frequency is shown by event magnitude (cm) for all event occurrences and for those events falling within the top 5% of ablation events.

Month	Extreme events	Extreme event magnitude (cm)			
		$3.0 \leq X < 4.5$	$4.5 \leq X < 6.0$	$6.0 \leq X < 9.0$	$X \geq 9.0$
Nov	8	7	0	1	0
Dec	29	20	5	3	1
Jan	43	26	12	2	3
Feb	67	37	20	8	2
Mar	61	37	17	6	1
Apr	3	2	1	0	0

for each SWC are presented in Fig. 6, and daily averaged meteorological conditions in Philadelphia for each SWC are available in Table 2. Meteorological conditions for each individual synoptic weather type are provided as Table S1 in the online supplemental material.

High pressure overhead (HOV) synoptic weather types exhibited a relative high pressure center in the general vicinity of the SRB (Fig. 6a), with an average magnitude of 1024 hPa (Table 2). During HOV types, the basin typically received clear-sky conditions and relatively moderate air temperatures based on the season of occurrence, except when the configuration of

high pressure resulted in winds from the east, where flow from the Atlantic Ocean likely resulted in orographically induced uplift and greater cloud cover relative to the other HOV types (Table 2). Wind directions for these types were variable during the day and exhibited the slowest average wind speeds of any of the SWCs at 2.2 m s^{-1} (Table 2). HOV types accounted for 23.8% of November–April days during the 1960–2009 study period, the second largest percentage of the five SWCs.

Northwest flow (NWF) types were associated with relatively high pressure to the west and relatively low pressure to the east, such that surface winds were from the west, northwest, or

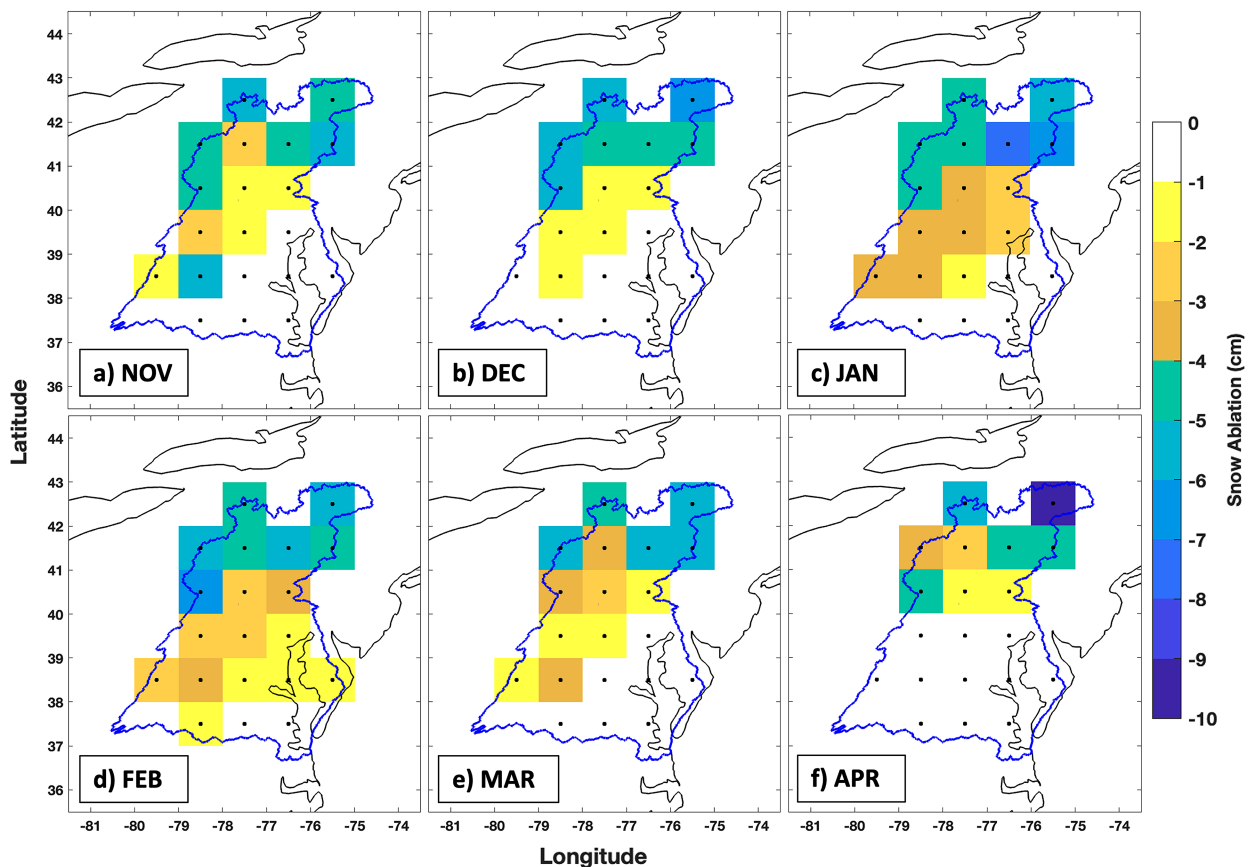


FIG. 5. Spatial distribution of snow magnitude ablated within the broader Chesapeake Basin (including SRB), in centimeters, during extreme ablation events, 1960–2009. Note that the number of days used in calculating this average differs by month, with November–April having 8, 29, 43, 67, 61, and 3 days, respectively.

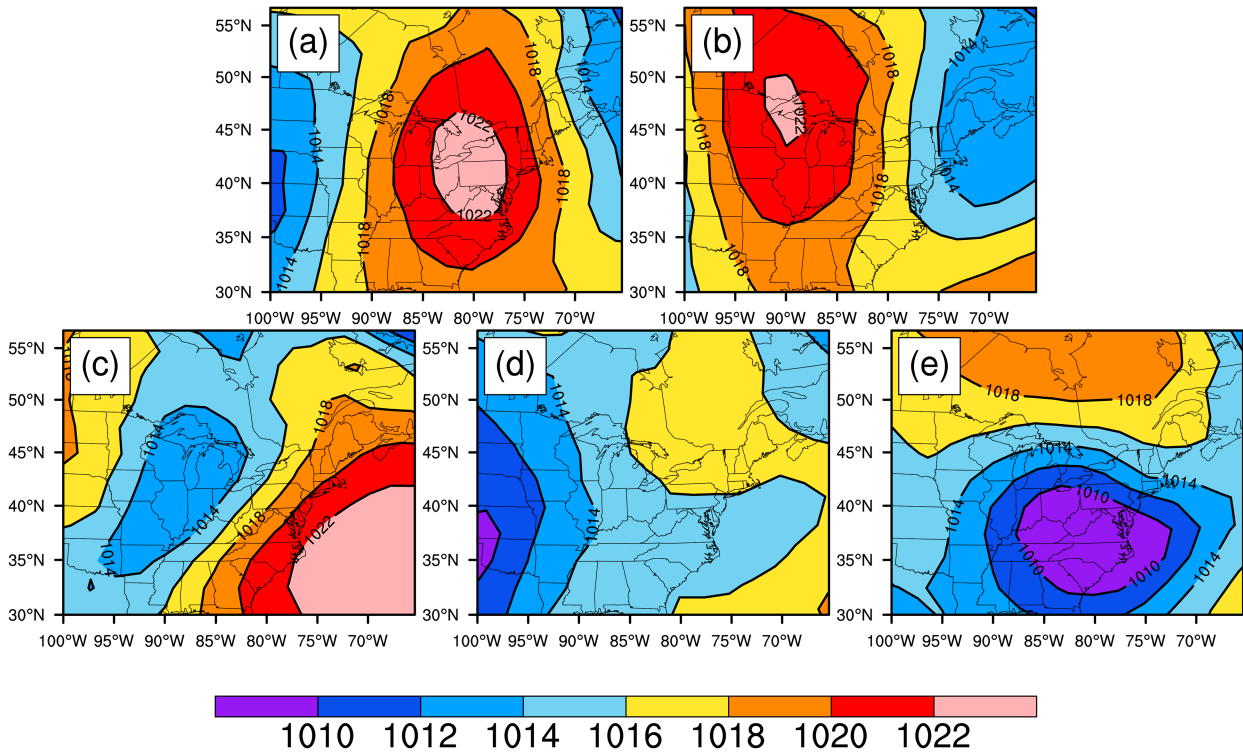


FIG. 6. Average sea level pressure field (hPa) for the eastern United States for a synoptic weather type representative of the five SWCs leading to ablation in the SRB: (a) HOV, (b) NWF, (c) SF, (d) WF, and (e) ROS.

north and typically advected cool and dry air into the SRB (Fig. 6b). This advection was evident within the composited meteorological conditions, with NWF types having the lowest air and dewpoint temperatures of the five SWCs, at 2.2° and -5.5°C , respectively (Table 2). Average wind speeds were the greatest for NWF types of the SWCs, with an average daily magnitude of 4.5 m s^{-1} (Table 2). These types were often preceded by a low pressure system tracking northeast along the eastern United States coast or in southern Quebec, Canada. NWF types were the most common of the SWCs, occurring 3786 times during the 50-yr study period and representing 27.7% of the total November–April days.

Southerly flow (SF) types exhibited a sea level pressure configuration that was the opposite of NWF types, with high pressure to the east and low pressure to the west (Fig. 6c). This configuration resulted in the advection of relatively warm and sometimes moist air from the southwest, south,

and/or southeast in the SRB (Table 2). Air temperatures during SF types were the highest, on average, of the SWCs at 6.9°C , while dewpoint temperatures were the second highest at 1.5°C (Table 2). SF types were the third most frequent SWC, accounting for 12.5% of days during the study period.

Weak flow (WF) synoptic weather types typically entailed a nondescript sea level pressure pattern with relatively weak and disorganized flow (Fig. 6d). However, depending on the direction of flow, this can result in the advection of relatively warm and moist air masses into the basin that can contribute to ablation (Table 2). These types represented approximately 9.9% of days in the November–April study period.

The rain-on-snow (ROS) types do not necessarily have a consistent synoptic-scale pattern, but rather, are conditions when liquid precipitation occurs within the SRB. ROS types are most often represented by a midlatitude cyclone tracking through or just north of the SRB, resulting in the advection of

TABLE 2. Average meteorological conditions at the Philadelphia TSI location for the five SWCs.

SWC	Air temperature ($^{\circ}\text{C}$)	Dewpoint temperature ($^{\circ}\text{C}$)	Sea level pressure (hPa)	Wind direction ($^{\circ}$)	Wind speed (m s^{-1})	Cloud cover (10ths)
HOV	4.9	-1.2	1024	339	2.2	6.0
NWF	2.2	-5.5	1019	303	4.5	3.7
SF	6.9	1.5	1018	220	2.2	7.3
WF	3.8	-1.3	1013	319	4.0	8.4
ROS	5.3	1.6	1009	63	3.6	8.8

TABLE 3. Average snow extreme ablation and extreme stream discharge magnitude per event and total frequency of extreme events in the SRB, 1960–2009. Ablation magnitude is shown as a negative value, indicative of snow loss.

SWC	Ablation event magnitude (cm)	Ablation event frequency (days)	Discharge event magnitude ($\text{ft}^3 \text{s}^{-1}$)	Discharge event frequency (days)
HOV	−4.9	62	147 064	58
NWF	−4.2	29	128 506	23
SF	−4.3	74	145 791	88
WF	−4.7	28	148 147	22
ROS	−5.8	14	130 115	55

warm and moist air from the south, cloud formation, and precipitation, potentially in association with a warm or cold front (Fig. 6e). ROS types had the highest dewpoint temperatures, cloudiest conditions, and lowest sea level pressure of the five SWCs at the Philadelphia TSI location (Table 2). ROS types were the least frequent of the SWCs, occurring just 20.6 days per year, or 7.5% days during the 50 yr.

c. Synoptic weather types and extreme ablation and discharge events

The 27 individual synoptic weather types within the five SWCs represented 98.1% of the extreme ablation events and 92.9% of the extreme discharge events within the 50-yr November–April season study period (Table S2 in the online supplemental material). HOV types resulted in 30.0% of SRB extreme ablation events, with an average magnitude of 4.9 cm of snow depth loss per event. As such, HOV types resulted in the second largest ablation magnitude and second highest frequency of ablation of the five SWCs (Table 3; Fig. 7). Similarly, HOV types accounted for the second highest frequency of extreme discharge events, at 23.6%. The average magnitude of a discharge event was approximately $147\,064 \text{ ft}^3 \text{ s}^{-1}$ (428% increase over long-term mean flow), the third largest of the SWCs (Table 3; Fig. 7).

NWF types resulted in approximately 14.0% of the 1960–2009 extreme ablation events and an average of 4.2 cm of snow depth loss per event, the lowest of the SWCs (Table 3; Fig. 7). A total of

23 extreme discharge events were associated with NWF (9.3%), with an average magnitude of approximately $128\,506 \text{ ft}^3 \text{ s}^{-1}$ (374% increase over long-term mean flow; Table 3; Fig. 7). NWF types, which often follow coastal storms, have the lowest average discharge magnitude of the SWCs.

In contrast to NWF types, SF types resulted in the most snow extreme ablation events within the basin at 35.7% and an average ablation magnitude of 4.3 cm (Table 3; Fig. 7). Extreme discharge events during SF types were approximately $145\,791 \text{ ft}^3 \text{ s}^{-1}$ (425% increase over long-term mean flow), and SF types accounted for 35.8% of the extreme discharge events, the most of the SWCs (Table 3; Fig. 7).

WF types resulted in 13.5% of the extreme SRB ablation events, with an average magnitude of 4.7 cm (Table 3; Fig. 7). These types resulted in the fewest extreme discharge events of the SWCs at 22 (8.9%), with an average daily magnitude of approximately $148\,147 \text{ ft}^3 \text{ s}^{-1}$ (432% increase over long-term mean flow; Table 3; Fig. 7).

ROS types resulted in just 6.8% of the extreme SRB ablation events; however, the average ablation magnitude for ROS types was 5.8 cm of snow depth loss, the most of the five SWCs (Table 3; Fig. 7). ROS types represented 22.4% of extreme discharge events during the 50-yr study period, with an average daily discharge of approximately $130\,115 \text{ ft}^3 \text{ s}^{-1}$ (379% increase over long-term mean flow; Table 3; Fig. 7).

d. Large-scale forcing mechanisms

During the November–April study period, the interannual frequency of all five SWCs was significantly related to the phase of at least one teleconnection index. HOV synoptic weather types were more frequent during years when the PNA was negatively phased (correlation $R = -0.321$; significance $p = 0.023$). NWF types were more frequent during years when the AMO was negatively phased ($R = -0.366$; $p = 0.002$). SF types were positively correlated with both the NAO and the AO ($R = 0.343$; $p = 0.015$ and $R = 0.332$; $p = 0.019$, respectively), indicating the types were more frequent when the indices were in their positive phases. The opposite correlation was evident for WF synoptic weather types, with WF types being more frequent when the NAO was negatively phased ($R = -0.295$; $p = 0.038$) and when the Niño-3.4 ENSO index was cooler than normal ($R = -0.285$; $p = 0.045$). The frequency of ROS weather types was significantly correlated with the AO ($R = -0.307$; $p = 0.030$), the Niño-3.4 ENSO index ($R = 0.379$; $p = 0.007$), the PDO ($R = 0.428$; $p = 0.002$), and the PNA ($R = 0.549$; $p < 0.001$). Correlation results of teleconnection indices and individual synoptic weather types are available in

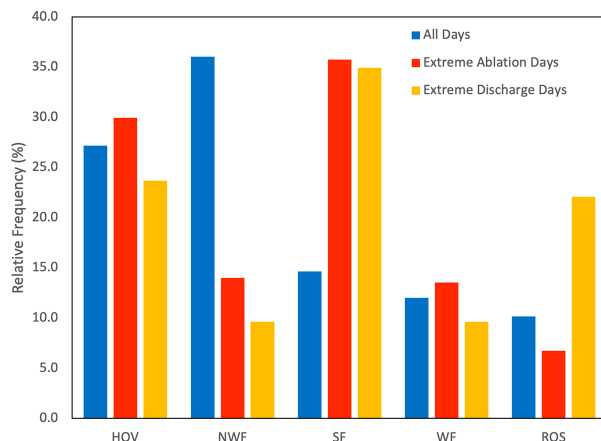


FIG. 7. Relative frequency (%) of the SWCs for all November–April days (blue), extreme ablation events (red), and extreme discharge events (yellow) from 1960 to 2009.

Table S3 in the online supplemental material but are not the point of emphasis in this paper.

4. Discussion

a. Climatology of extreme ablation and discharge events

Similar to prior research in the SRB and the surrounding region (Leathers et al. 2004; Wachowicz et al. 2020; Suriano et al. 2021; Welty and Zeng 2021), snow ablation is observed to be most common during the late winter and early spring months of February and March. This corresponds well to peak snowpack depth and the onset of warmer and more humid atmospheric conditions while exiting the cold season (Hatchett et al. 2022) and when there is the greatest frequency of extreme discharge events in the basin. By narrowing the scope of ablation events analyzed here to extreme events (top 5% of the distribution), we note a modest increase in the percentage of ablation events generating a positive (increasing) response in river discharge from 75.6% with events of at least 2.54 cm (Suriano et al. 2020) to 87.7% here. This suggests that larger ablation events are more likely to yield enhanced runoff relative to smaller events, based on more water likely being available within the pack. Despite the various other factors that can influence runoff, the magnitude of snow ablation is a major contributor during the cold season.

Leathers et al. (2008) developed a long-term hydroclimatic reconstruction of the Susquehanna River basin that included analysis of mean annual flow. They found for the period 1680–2006, mean annual flow of the Susquehanna River was $34\,326\text{ ft}^3\text{ s}^{-1}$. In comparison, an extreme discharge event here represents 412% of that long-term mean annual flow. Over half of the extreme discharge events in the basin occur during the cold season in association with an ablation event, while approximately 25% occurred during the cool season but were not linked directly to ablation here. The remaining approximately 20% of extreme discharge events occur during the warm season (May–September), associated with heavy and often widespread precipitation events such as those found with remnants of tropical systems [e.g., Agnes in 1972 (Toomey et al. 2019) and Lee in 2011 (Kochel et al. 2016)].

While this research did not evaluate changes in extreme discharge over time, other efforts have explored this in greater detail. When evaluating potential changes in discharge in response to a changing climate, findings report projected increases in annual streamflow by some 24% in the twenty-first century (Najjar 1999), while mean annual peak discharge decreases as snowfall reduces with warmer winter temperatures (Ray et al. 2016). When determining the criteria for including data, the top 5%, top 10%, and top 15% of discharge events and ablation events were initially considered. When results were compared for all three, the increase in accuracy due to the increase in the number of data points across the percentiles was countered by the loss of emphasis on extreme ablation events, one of the main points of this study (figures not shown).

b. Synoptic weather types

The relative frequencies of the five SWCs were similar to that reported in other studies focused in the broader Northeast

and/or mid-Atlantic. Siegert et al. (2021) also identifies southerly/southwesterly flow, northwest flow, and high pressure overhead types as the most common patterns leading to streamflow in forested watersheds in the Northeast. While they find southwesterly flow types were associated with 37% of streamflow events, the study was focused on the warm season and acknowledges the types were least common during the winter season with average interannual frequencies in line with values reported here. Also focused on the SRB, Miller et al. (2006) analyzed synoptic patterns in association with spring discharge events, finding 10 primary patterns, including Bermuda Highs, Ohio Valley Highs, and Nor'easters, that are highly similar to SWCs identified here.

Based on prior research, it is likely that each of the primary five SWCs initiates ablation from different combinations of latent, sensible, and radiative transfer into the snowpack. Using the nearby Great Lakes basin as a comparison with the SRB (e.g., Suriano and Leathers 2018), HOV types commonly ablate snow due to relatively high levels of shortwave radiation associated with clear-sky conditions and occasionally with moderate fluxes of sensible heat. Here, we note that while some HOV types appear to meet this description, two of them (HOV_A_1 and HOV_W_1) indicate overcast skies are observed in Philadelphia when the patterns occur. These two patterns' high sea level pressure center is located just north of the SRB (not shown); thus, wind flow is predominantly easterly and likely results in topographically induced uplift of relatively moist maritime air masses from the Atlantic Ocean. This mechanism of ablation would be more heavily influenced by latent and sensible heat transfers, similar to SF types (see below), despite the prevalence of high pressure over the SRB.

NWF types typically ablate snow via a variety of mechanisms, including enhanced latent and sensible fluxes associated with a frontal passage through the region at the very beginning of the calendar day and/or the very end of the previous day (Suriano and Leathers 2018). This passage is typically linked to a midlatitude cyclone to the north and east where the daily composite indicates northwest flow is the dominant regime. Lower levels of cloud cover following this frontal passage also enhance shortwave fluxes into the snowpack and can lead to moderate levels of ablation (Suriano and Leathers 2018).

SF types typically ablate snow in the U.S. Northeast and Midwest primarily via sensible and latent heat fluxes driven by the strong advection of warm, and sometimes moist, air from the south (Suriano and Leathers 2018). The presence of cloud cover can also aid in the retention of longwave radiation aiding in ablation, while also lessening the magnitude of energy received via shortwave radiation (Suriano and Leathers 2018). WF types have a less-clear pathway of driving ablation due to the varied configurations of sea level pressure and general low pressure gradients observed. This is further evident by the “middle of the road” average meteorological characteristics of WF types relative to the other four SWCs (see Table 2).

ROS types within the mid-Atlantic typically ablate snow via turbulent fluxes associated with relatively high air temperatures, dewpoint temperatures, and wind speeds (Wachowicz et al. 2020; Grote 2021). Inherent to ROS types is also the

energy imparted to the snowpack by the precipitation itself; the rain imparts sensible heat due to its above-freezing temperature, and latent heat is often released into the snowpack when the rain freezes within it. Case studies indicate some 85% of the net energy into the snowpack during ROS within the SRB are from turbulent heat fluxes, with sensible heat alone being responsible for nearly 55% of the net energy flux into the snowpack (Leathers et al. 1998). Grote (2021) further describes the role of the low-level jet in advecting warm air and moist air from the Gulf of Mexico and/or Atlantic Ocean as prime atmospheric conditions for ROS-induced flooding in the mid-Atlantic.

c. Synoptic weather types and extreme ablation and discharge events

Our results found that SF types represented the largest relative frequency of both extreme ablation and extreme discharge events during the study period, similar to research from the surrounding region (Suriano 2019, 2020; Leathers et al. 2004; Welty and Zeng 2021). Suriano (2019) evaluated atmospheric mechanisms for snow ablation, not restricted to only extreme events, and notes that classified SF synoptic types represented from 23% of ablation in the Lake Ontario basin to nearly 44% of events in the Lake Huron basin. When examining the most extreme ablation events in the Great Lakes basin, Suriano (2020) identifies that 63.6% of events are attributed to SF types. Leathers et al. (2004) used air masses as a means to analyze ablation events in the central Appalachians, finding ablation was most common during instances of moist moderate, dry moderate, and moist polar air-mass types. Leathers et al. (2004) also indicates atmospheric conditions resulting in southerly flow into the region were responsible for the largest percentage of ablation events, noting instances of liquid precipitation led to some of the highest rates of ablation. Furthermore, Welty and Zeng (2021) identify an enhanced 500-hPa trough over the western Great Plains as prime conditions for ablation in the Northeast (inclusive of the SRB). This would place the ascending branch of the 500-hPa trough over the Midwest United States and favor the development of midlatitude cyclones to the immediate west of the SRB. Such a development closely resembles the composite maps of the SF types leading to ablation here.

The largest-magnitude ablation events, on average, were associated with ROS types over the study period, and ROS was the third highest percentage of extreme discharge events (behind SF and HOV types). This mirrors results noted elsewhere in eastern North America where ROS are typically observed to result in the larger magnitudes of ablation per event relative to non-ROS events (e.g., Suriano and Leathers 2018). Where results differ here with the literature is in the relative frequency of ROS events. Here we note that less than 10% of extreme ablation events are associated with ROS types. Elsewhere, ROS ablation has been evaluated as approximately 28% of events in the Northeast (Welty and Zeng 2021), from 24% (Welty and Zeng 2021) to 27% (Suriano and Leathers 2018) in the Great Lakes basin, and approximately 30% broadly in the mid-Atlantic (Suriano 2022). The underrepresentation of ROS

noted here could be due to a variety of factors, such as the specific definition of ablation used, the focus here on “extreme” events, and the type of dataset used (observed versus modeled product). Such a discrepancy may also be due to how a ROS event is defined, as discussed in Wachowicz et al. (2020). Further, ROS synoptic weather types are inherently not a specific synoptic weather type in the same sense that a pattern resulting in westerly flow or a high pressure center overhead is. As such, there is some level of researcher-specific subjectivity in identifying such a pattern and the potential for variations in results in relative frequency of occurrence.

d. Large-scale forcing mechanisms

With the relative frequency of multiple SWCs being significantly correlated with the phases of large-scale teleconnection indices, it is prudent to discuss the physical mechanism(s) that support such statistical linkages. Some of the strongest correlations were observed with the PNA. Under a positively phased PNA, there is enhanced troughing over the eastern United States and Atlantic coast at midlevels of the atmosphere (Leathers and Palecki 1992). As such, one would expect to see a greater frequency of midlatitude cyclones tracking up the Eastern Seaboard and along the spine of the Appalachians in agreement with the ascending branch of the trough favoring upper-level divergence and low pressure formation at the surface. This aligns with the atmospheric conditions in which the ROS SWC occurs, placing the SRB within the warm sector of the cyclone and increasing the potential for liquid precipitation to occur. Conversely, a negatively phased PNA would indicate the opposite configuration, with enhanced ridging in the eastern United States, placing the descending branch of the midlevel wave train, and associated convergence and surface high pressure, over the mid-Atlantic region inclusive of the SRB, as seen here with the HOV types.

Although with slightly different mechanisms, the AO and NAO indices are similar with respect to their impacts on upper-level circulation over North America. When the indices are negatively phased, there is an increased tendency for upper-level troughing over the eastern United States, similar to that of a positive PNA. Conversely, a positive AO/NAO favors the development of low pressure to the west of the SRB, in the Midwest, and relatively higher pressure off the Atlantic coast through the configuration of mid- to upper-level patterns. This gives rise to an enhanced frequency of SF types. The frequencies of WF types and ROS types were oppositely related to the Niño-3.4 ENSO index, such that when ocean temperatures were warmer, WF types were less frequent and ROS types were more frequent. The positive correlation between the Niño-3.4 ENSO index and ROS types' frequency is similar to that observed in the U.S. Southwest (McCabe et al. 2007), supported by enhanced precipitation anomalies during El Niño events in these regions. While this study did not emphasize temporal trends in ablation, discharge, or SWCs' frequency, evaluation of the physical forcing mechanisms of these variables can prove valuable in understanding potential future changes in their occurrence.

5. Conclusions

This study evaluated the climatology of extreme snow ablation and extreme river discharge events within the Susquehanna River basin over a 50-yr period. Using a synoptic classification technique, particular emphasis was placed on resolving the synoptic-scale weather patterns that are associated with ablation and discharge events within the basin and how global-scale modes of variability are related to their interannual frequency. Extreme snow ablation events, representing the top 5% of the distribution by magnitude, were observed in each month of the November–April study season; however, they were most frequent during March and February. Per extreme event, approximately 4.5 cm of basinwide areal-weighted snow depth was ablated on average, and an extreme discharge event for the basin was over $141\,000\text{ ft}^3\text{ s}^{-1}$ on average. This increase in discharge represents a 412% increase from the long-term mean flow.

Extreme events, both ablation and discharge, most commonly occurred during synoptic-scale weather types of southerly flow. Such weather types are typically associated with the advection of warm and often moist air masses into the basin with moderate to relatively strong wind speeds, requisite meteorological conditions for rapid ablation. While relatively infrequent, instances of rain-on-snow led to the largest magnitude of ablation per event and are also associated with large latent and sensible heat fluxes. The frequency of such ROS weather types was significantly correlated with the phase of the PNA, where ROS types were more frequent during winter seasons when the PNA was positively phased.

Further research into the role of atmospheric variations in driving ablation events in the eastern United States is warranted. While not evaluated in this study, preliminary evidence suggests the interannual frequency and the internal meteorological characteristics of ablation-causing synoptic weather types have changed over time. Such changes alter the potential for ablation events to occur in the region and may impact the intensity of events in the future. Particular emphasis on ROS events for future research is proposed, given the regional hydroclimatology and potential for change in the remaining twenty-first century.

Acknowledgments. The authors do not have any conflicts of interests that are not apparent from their listed affiliation. Tina Callahan at the University of Delaware is acknowledged for her assistance in generating Fig. 1.

Data availability statement. Data used in this study are freely available at the National Snow and Ice Data Center (<https://doi.org/10.7265/N5028PQ3>; T. L. Mote et al. 2018).

REFERENCES

- Anderson, D. M., P. M. Glibert, and J. M. Burkholder, 2002: Harmful algal blooms and eutrophication: Nutrient sources, composition, and consequences. *Estuaries*, **25**, 704–726, <https://doi.org/10.1007/BF02804901>.
- Anderson, E. A., 1976: A point energy and mass balance model of snow cover. NOAA Tech. Rep. NWS 19, 150 pp., https://repository.library.noaa.gov/view/noaa/6392/noaa_6392_DS1.pdf.
- Barnett, T. P., J. C. Adam, and D. P. Lettenmaier, 2005: Potential impacts of a warming climate on water availability in snow-dominated regions. *Nature*, **438**, 303–309, <https://doi.org/10.1038/nature04141>.
- Barnston, A. G., and R. E. Livezey, 1987: Classification, seasonality and persistence of low-frequency atmospheric circulation patterns. *Mon. Wea. Rev.*, **115**, 1083–1126, [https://doi.org/10.1175/1520-0493\(1987\)115<1083:CSAPOL>2.0.CO;2](https://doi.org/10.1175/1520-0493(1987)115<1083:CSAPOL>2.0.CO;2).
- Bednorz, E., 2009: Synoptic conditions for rapid snowmelt in the Polish-German lowlands. *Theor. Appl. Climatol.*, **97**, 279–286, <https://doi.org/10.1007/s00704-008-0063-z>.
- Broxton, P., X. Zeng, and N. Dawson, 2019: Daily 4 km gridded SWE and snow depth from assimilated in-situ and modeled data over the conterminous US, version 1. NASA National Snow and Ice Data Center, accessed 15 August 2022, <https://doi.org/10.5067/0GGPB220EX6A>.
- Changnon, S. A., 2008: Assessment of flood losses in the United States. *J. Contemp. Water Res. Educ.*, **138**, 38–44, <https://doi.org/10.1111/j.1936-704X.2008.00007.x>.
- Cohen, J., H. Ye, and J. Jones, 2015: Trends and variability in rain-on-snow events. *Geophys. Res. Lett.*, **42**, 7115–7122, <https://doi.org/10.1002/2015GL065320>.
- Dèry, S., and M. Yau, 2002: Large-scale mass balance effects of blowing snow and surface sublimation. *J. Geophys. Res.*, **107**, 4679, <https://doi.org/10.1029/2001JD001251>.
- Dyer, J. L., and T. L. Mote, 2007: Trends in snow ablation over North America. *Int. J. Climatol.*, **27**, 739–748, <https://doi.org/10.1002/joc.1426>.
- Enfield, D. B., A. M. Mestas-Nunez, and P. J. Trimble, 2001: The Atlantic multidecadal oscillation and its relation to rainfall and river flows in the continental U.S. *Geophys. Res. Lett.*, **28**, 2077–2080, <https://doi.org/10.1029/2000GL012745>.
- Frei, A., R. L. Armstrong, M. P. Clark, and M. C. Serreze, 2002: Catskill Mountain water resources vulnerability, hydroclimatology, and climate-change sensitivity. *Ann. Assoc. Amer. Geogr.*, **92**, 203–224, <https://doi.org/10.1111/1467-8306.00287>.
- Fritze, H., I. T. Stewart, and E. Pebesma, 2011: Shifts in western North American snowmelt runoff regimes for the recent warm decades. *J. Hydrometeorol.*, **12**, 989–1006, <https://doi.org/10.1175/2011JHM1360.1>.
- Grote, T., 2021: A synoptic climatology of rain-on-snow flooding in mid-Atlantic region using NCEP/NCAR re-analysis. *Phys. Geogr.*, **42**, 452–471, <https://doi.org/10.1080/02723646.2020.1838119>.
- Grundstein, A. J., and D. J. Leathers, 1999: A spatial analysis of snow–surface energy exchanges over the northern Great Plains of the United States in relation to synoptic scale forcing mechanisms. *Int. J. Climatol.*, **19**, 489–511, [https://doi.org/10.1002/\(SICI\)1097-0088\(199904\)19:5<489::AID-JOC373>3.0.CO;2-J](https://doi.org/10.1002/(SICI)1097-0088(199904)19:5<489::AID-JOC373>3.0.CO;2-J).
- Guan, B., D. E. Waliser, F. M. Ralph, E. J. Fetzer, and P. J. Neiman, 2016: Hydrometeorological characteristics of rain-on-snow events associated with atmospheric rivers. *Geophys. Res. Lett.*, **43**, 2964–2973, <https://doi.org/10.1002/2016GL067978>.
- Haleakala, K., M. Gebremichael, J. Dozier, and D. P. Lettenmaier, 2021: Factors governing winter snow accumulation and ablation susceptibility across the Sierra Nevada (United States). *J. Hydrometeorol.*, **22**, 1455–1472, <https://doi.org/10.1175/JHM-D-20-0257.1>.

- Hatchett, B. J., A. M. Rhoades, and D. J. McEvoy, 2022: Monitoring the daily evolution and extent of snow drought. *Nat. Hazards Earth Syst. Sci.*, **22**, 869–890, <https://doi.org/10.5194/nhess-22-869-2022>.
- Higgins, R. W., A. Leetmaa, Y. Xue, and A. G. Barnston, 2000: Dominant factors influencing the seasonal predictability of U.S. precipitation and surface air temperature. *J. Climate*, **13**, 3994–4017, [https://doi.org/10.1175/1520-0442\(2000\)013<3994:DFITSP>2.0.CO;2](https://doi.org/10.1175/1520-0442(2000)013<3994:DFITSP>2.0.CO;2).
- Kalkstein, L. S., and P. Corrigan, 1986: A synoptic climatological approach for geographical analysis: Assessment of sulfur dioxide concentrations. *Ann. Assoc. Amer. Geogr.*, **76**, 381–395, <https://doi.org/10.1111/j.1467-8306.1986.tb00126.x>.
- , G. Tan, and J. A. Skindlov, 1987: An evaluation of three clustering procedures for use in synoptic climatological classification. *J. Climate Appl. Meteor.*, **26**, 717–730, [https://doi.org/10.1175/1520-0450\(1987\)026<0717:AEOTCP>2.0.CO;2](https://doi.org/10.1175/1520-0450(1987)026<0717:AEOTCP>2.0.CO;2).
- Kalnay, E., and Coauthors, 1996: The NCEP/NCAR 40-Year Reanalysis Project. *Bull. Amer. Meteor. Soc.*, **77**, 437–471, [https://doi.org/10.1175/1520-0477\(1996\)077<0437:TNYRP>2.0.CO;2](https://doi.org/10.1175/1520-0477(1996)077<0437:TNYRP>2.0.CO;2).
- Kluver, D., T. L. Mote, D. J. Leathers, G. R. Henderson, W. Chan, and D. A. Robinson, 2017: Creation and validation of a comprehensive 1° by 1° daily gridded North American dataset for 1900–2009: Snowfall. *J. Atmos. Oceanic Technol.*, **33**, 857–871, <https://doi.org/10.1175/JTECH-D-15-0027.1>.
- Kochel, R. C., B. R. Hayes, J. Muhlbauer, Z. Hancock, and D. Rockwell, 2016: Intersection of fluvial disequilibrium and legacy of logging. *Geosphere*, **12**, 305–345, <https://doi.org/10.1130/GES01180.1>.
- Leathers, D. J., and M. A. Palecki, 1992: The Pacific/North American teleconnection pattern and United States climate. Part II: Temporal characteristics and index specification. *J. Climate*, **5**, 707–716, [https://doi.org/10.1175/1520-0442\(1992\)005<0707:TPATPA>2.0.CO;2](https://doi.org/10.1175/1520-0442(1992)005<0707:TPATPA>2.0.CO;2).
- , B. Yarnal, and M. A. Palecki, 1991: The Pacific/North American teleconnection pattern and United States climate. Part I: Regional temperature and precipitation associations. *J. Climate*, **37**, 4962–4971, [https://doi.org/10.1175/1520-0442\(1991\)004<0517:TPATPA>2.0.CO;2](https://doi.org/10.1175/1520-0442(1991)004<0517:TPATPA>2.0.CO;2).
- , T. Kluck, and S. Kroczyński, 1998: The severe flooding event of 1996 across north-central Pennsylvania. *Bull. Amer. Meteor. Soc.*, **79**, 785–797, [https://doi.org/10.1175/1520-0477\(1998\)079<0785:TSFE0J>2.0.CO;2](https://doi.org/10.1175/1520-0477(1998)079<0785:TSFE0J>2.0.CO;2).
- , D. Y. Graybeal, T. L. Mote, A. J. Grundstein, and D. A. Robinson, 2004: The role of airmass types and surface energy fluxes in snow cover ablation in the central Appalachians. *J. Appl. Meteor.*, **43**, 1887–1898, <https://doi.org/10.1175/JAM2172.1>.
- , M. L. Malin, D. B. Kluver, G. R. Henderson, and T. A. Bogart, 2008: Hydroclimatic variability across the Susquehanna River basin, USA, since the 17th century. *Int. J. Climatol.*, **28**, 1615–1626, <https://doi.org/10.1002/joc.1668>.
- Li, D., M. L. Wrzesien, A. J. Durand, and D. P. Lettenmaier, 2017: How much runoff originates as snow in the western United States, and how will that change in the future? *Geophys. Res. Lett.*, **44**, 6163–6172, <https://doi.org/10.1002/2017GL073551>.
- Lindsay, R., M. Wensahan, A. Schweiger, and J. Zhang, 2013: Evaluation of seven different atmospheric reanalysis products in the Arctic. *J. Climate*, **27**, 2588–2606, <https://doi.org/10.1175/JCLI-D-13-00014.1>.
- Mazurkiewicz, A. B., D. G. Callery, and J. J. McDonnell, 2008: Assessing the controls of the snow energy balance and water available for runoff in a rain-on-snow environment. *J. Hydrol.*, **354**, 1–14, <https://doi.org/10.1016/j.jhydrol.2007.12.027>.
- McCabe, G., M. Clark, and L. Hay, 2007: Rain-on-snow events in the western United States. *Bull. Amer. Meteor. Soc.*, **88**, 319–328, <https://doi.org/10.1175/BAMS-88-3-319>.
- Miller, W. D., D. G. Kimmel, and L. W. Harding Jr., 2006: Predicting spring discharge of the Susquehanna River from a winter synoptic climatology for the eastern United States. *Water Resour. Res.*, **42**, W05414, <https://doi.org/10.1029/2005WR004270>.
- Mote, P. W., S. Li, D. P. Lettenmaier, M. Xiao, and R. Engel, 2018: Dramatic declines in snowpack in the western US. *npj Climate Atmos. Sci.*, **1**, 2, <https://doi.org/10.1038/s41612-018-0012-1>.
- Mote, T. L., T. W. Estilow, G. R. Henderson, D. J. Leathers, D. A. Robinson, and Z. J. Suriano, 2018: Daily gridded North American snow, temperature, and precipitation, 1959–2009, version 1. National Snow and Ice Data Center, accessed 22 September 2023, <https://doi.org/10.7265/N5028PQ3>.
- Musselman, K. N., N. Addor, J. A. Vano, and N. P. Molotch, 2021: Winter melt trends portend widespread declines in snow water resources. *Nat. Climate Change*, **11**, 418–424, <https://doi.org/10.1038/s41558-021-01014-9>.
- Najjar, R. G., 1999: The water balance of the Susquehanna River basin and its response to climate change. *J. Hydrol.*, **219**, 7–19, [https://doi.org/10.1016/S0022-1694\(99\)00041-4](https://doi.org/10.1016/S0022-1694(99)00041-4).
- Pradhanang, S. M., A. Anandhi, R. Mukundan, M. S. Zion, D. C. Pierson, E. M. Schneiderman, A. Matonse, and A. Frei, 2011: Application of SWAT model to assess snowpack development and streamflow in the Cannonsville watershed, New York, USA. *Hydrol. Processes*, **25**, 3268–3277, <https://doi.org/10.1002/hyp.8171>.
- Ray, R. L., R. E. Beighley, and Y. Yoon, 2016: Integrating runoff generation and flow routing in Susquehanna River basin to characterize key hydrologic processes contributing to maximum annual flood events. *J. Hydrol. Eng.*, **21**, 04016026, [https://doi.org/10.1061/\(ASCE\)HE.1943-5584.0001389](https://doi.org/10.1061/(ASCE)HE.1943-5584.0001389).
- Robinson, D. A., 1988: Construction of a United States historical snow database. *Proc. 45th Eastern Snow Conf.*, Lake Placid, NY, Eastern Snow Conference, 50–59, https://climate.rutgers.edu/stateclim_v1/robinson_pubs/refereed/Robinson_1988.pdf.
- Siebert, C. M., D. J. Leathers, and D. F. Levia, 2017: Synoptic typing: Interdisciplinary application methods with three practical hydroclimatological examples. *Theor. Appl. Climatol.*, **128**, 603–621, <https://doi.org/10.1007/s00704-015-1700-y>.
- , and Coauthors, 2021: Effects of atmospheric circulation on stream chemistry in forested watersheds across the north-eastern United States: Part 1. Synoptic-scale forcing. *J. Geophys. Res. Atmos.*, **126**, e2020JD033413, <https://doi.org/10.1029/2020JD033413>.
- Siirila-Woodburn, E. R., and Coauthors, 2021: A low-to-no snow future and its impacts on water resources in the western United States. *Nat. Rev. Earth Environ.*, **2**, 800–819, <https://doi.org/10.1038/s43017-021-00219-y>.
- Suriano, Z. J., 2019: On the role of snow cover ablation variability and synoptic-scale atmospheric forcings at the sub-basin scale within the Great Lakes watershed. *Theor. Appl. Climatol.*, **135**, 607–621, <https://doi.org/10.1007/s00704-018-2414-8>.
- , 2020: Synoptic and meteorological conditions during extreme snow cover ablation events in the Great Lakes basin. *Hydrol. Processes*, **34**, 1949–1965, <https://doi.org/10.1002/hyp.13705>.
- , 2022: North American rain-on-snow climatology. *Climate Res.*, **87**, 133–145, <https://doi.org/10.3354/cr01687>.

- , and D. J. Leathers, 2017: Spatiotemporal variability of Great Lakes basin snow cover ablation events. *Hydrol. Processes*, **31**, 4229–4237, <https://doi.org/10.1002/hyp.11364>.
- , and —, 2018: Great Lakes basin snow cover ablation and synoptic-scale atmospheric circulation. *J. Appl. Meteor. Climatol.*, **57**, 1497–1510, <https://doi.org/10.1175/JAMC-D-17-0297.1>.
- , G. R. Henderson, and D. J. Leathers, 2020: Discharge responses associated with rapid snow cover ablation events in the Susquehanna and Wabash River basins. *Phys. Geogr.*, **41**, 70–82, <https://doi.org/10.1080/02723646.2019.1674558>.
- , D. J. Leathers, T. L. Mote, G. R. Henderson, T. W. Estilow, L. J. Wachowicz, and D. A. Robinson, 2021: Declining North American snow cover ablation events. *Int. J. Climatol.*, **41**, 5213–5225, <https://doi.org/10.1002/joc.7125>.
- Toomey, M., and Coauthors, 2019: The mighty Susquehanna—Extreme floods in eastern North America during the past two millennia. *Geophys. Res. Lett.*, **46**, 3398–3407, <https://doi.org/10.1029/2018GL080890>.
- Wachowicz, L. J., T. L. Mote, and G. R. Henderson, 2020: A rain on snow climatology and temporal analysis for the eastern United States. *Phys. Geogr.*, **41**, 54–69, <https://doi.org/10.1080/02723646.2019.1629796>.
- Welty, J., and X. Zeng, 2021: Characteristics and causes of extreme snowmelt over the conterminous United States. *Bull. Amer. Meteor. Soc.*, **102**, 1526–1542, <https://doi.org/10.1175/BAMS-D-20-0182.1>.
- Yan, H., N. Sun, M. Wigmosta, R. Skaggs, L. R. Leung, A. Coleman, and Z. Hou, 2019: Observed spatiotemporal changes in the mechanisms of extreme water available for runoff in the western United States. *Geophys. Res. Lett.*, **46**, 767–775, <https://doi.org/10.1029/2018GL080260>.
- Yarnal, B., 1993: *Synoptic Climatology in Environmental Analysis: A Primer*. Belhaven Press, 195 pp.
- , D. L. Johnson, B. J. Frakes, G. I. Bowles, and P. Pascale, 1997: The flood of '96 and its socioeconomic impacts in the Susquehanna River basin. *J. Amer. Water Resour. Assoc.*, **33**, 1299–1312, <https://doi.org/10.1111/j.1752-1688.1997.tb03554.x>.
- Zhang, Y., J. M. Wallace, and D. S. Battisti, 1997: ENSO-like interdecadal variability: 1900–93. *J. Climate*, **10**, 1004–1020, [https://doi.org/10.1175/1520-0442\(1997\)010<1004:ELIV>2.0.CO;2](https://doi.org/10.1175/1520-0442(1997)010<1004:ELIV>2.0.CO;2).